

NMR in $^{55}\text{Mn}^{2+}$ nuclei in the quasi-one-dimensional antiferromagnetic CsMnBr_3

A. S. Borovik-Romanov,^{*} S. V. Petrov, and A. M. Tikhonov

Kapitsa Institute of Physics Problems, Russian Academy of Sciences, 117334 Moscow, Russia

B. S. Dumesh

Institute of Spectroscopy, Russian Academy of Sciences, 142092 Troitsk, Moscow Region, Russia

(Submitted 23 July 1997)

Zh. Éksp. Teor. Fiz. **113**, 352–368 (January 1998)

The NMR spectrum of the quasi-one-dimensional easy-plane antiferromagnetic CsMnBr_3 , which has trigonal spin lattice, is investigated in detail. The measurements were performed on a wide-band NMR decimeter microwave-band spectrometer over a wide range of magnetic fields at temperatures 1.3–4.2 K. All three branches of the NMR spectrum previously found by us [JETP Lett. **64**, 225 (1996)] are severely distorted because of the dynamic interaction with the Goldstone mode in the antiferromagnetic resonance spectrum. The experimental results in fields up to 40 kOe are described satisfactorily by an equation obtained by Zaliznyak *et al.* [JETP Lett. **64**, 473 (1996)]. Formulas are obtained in our work that agree very well with experiment at all fields up to the “collapse” field H_c of all sublattices. The unbiased NMR frequency in CsMnBr_3 is determined to be $\nu_{n0}=416$ MHz ($T=1.3$ K) in zero external magnetic field, and in this way the reduction in the spontaneous moment due to the quasi-one-dimensional nature of the system of Mn^{2+} spins, which according to our data amounts to 28%, is determined more accurately. The field dependences of the directions of the magnetic sublattices with respect to the magnetic field are obtained from the NMR spectra, confirming the equations of Chubukov [J. Phys. Condens. Matter **21**, 441 (1988)]. The results on the field dependence of the width and intensities of the NMR lines are discussed, along with three observed anomalies: 1) a strong increase in the NMR frequency for nuclei in sublattices that are perpendicular to the magnetic field; 2) the nonmonotonic temperature dependence of the resonance field for the lower branch of the spectrum; 3) the presence of two branches of the NMR spectrum in large H_c fields, in which the CsMnBr_3 must be a quasi-one-dimensional antiferromagnetic. © 1998 American Institute of Physics. [S1063-7761(98)02401-9]

1. INTRODUCTION

The quasi-one-dimensional antiferromagnetic CsMnBr_3 ($T_N=8.3$ K) has been vigorously investigated in recent years, both theoretically and experimentally. A number of extremely interesting properties have been found in the electron spin system of this material: quasi-one-dimensional exchange interaction and trigonal magnetic structure,¹ a phase transition to a quasicollinear structure in a comparatively weak magnetic field² H_c , and the electron susceptibility anisotropy^{3,4} associated with the latter, a large reduction in the electron spin moment,^{1,4} and the presence of the Goldstone mode in the antiferromagnetic resonance (AFMR) spectrum,^{5,6} the frequency of which is proportional to the cube of the magnetic field. This paper is devoted to an investigation of the unique features of the NMR spectrum of the nuclei of $^{55}\text{Mn}^{2+}$ magnetic ions, a brief observational description of which has been given elsewhere.⁷

There are several distinctive features of NMR in the nuclei of magnetic ions in antiferromagnetics.⁸ The NMR frequency of the nuclei of magnetic ions is determined primarily by the magnitude of the hyperfine field, which for the 3d elements is proportional to the average electron spin $\langle S \rangle$. In particular, for $^{55}\text{Mn}^{2+}$ ions this field can amount to 600–700 kOe. Accordingly, NMR is observed in $^{55}\text{Mn}^{2+}$ nuclei in

relatively weak fields at very high frequencies (up to 700 MHz).

A strong anisotropy of the exchange interaction (the ratio of the exchange integrals along the chains to their value perpendicular to the chains ≈ 500) is preserved in CsMnBr_3 despite the establishment of three-dimensional ordering. Therefore, a considerable reduction must occur in the mean spin $\langle S \rangle$ of the Mn^{2+} magnetic ion because of the presence of large quantum fluctuations induced by the quasi-one-dimensional nature of the exchange interaction. The NMR frequency at the nuclei of the magnetic ions in zero magnetic field, as we have pointed out, is determined by $\langle S \rangle$. Therefore, an investigation of the NMR spectrum is one of the most accurate methods of determining $\langle S \rangle$ and, accordingly, the reduction in the spin moment. Determination of the electron spin reduction in CsMnBr_3 was one of the goals of this work.

CsMnBr_3 is an easy-plane antiferromagnetic with trigonal magnetic structure. When an external magnetic field is applied in any direction in the easy plane, the NMR spectrum must split into three branches. By investigating the dependence of the resonance frequencies of these branches on the applied field, one can trace the transition of the trigonal antiferromagnetic structure into quasi-collinear. The second goal of our work was to investigate this process and to compare the data obtained with the prediction of the Chubukov

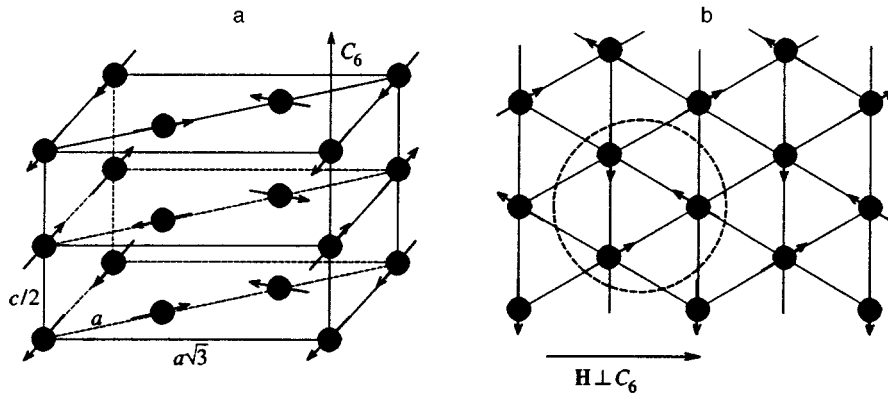


FIG. 1. Magnetic structure of the CsMnBr_3 antiferromagnetic (a—unit magnetic cell; b—orientation of spins in hexagonal plane with respect to the applied field \mathbf{H}).

theory.⁵ It must be pointed out that CsMnBr_3 is the first antiferromagnetic in which NMR could be observed in the nuclei of all sublattices forming the trigonal magnetic structure.

Another unique feature of the resonance properties of antiferromagnetics is associated with the strong correlation of the vibrations of the nuclei with the vibrations of the electron system. The effect of this correlation on the AFMR was first established by Heeger, Portis, Teaney and Witt,⁹ who found a strong temperature dependence for the location of the AFMR line in the KMnF_3 antiferromagnetic and observed a double electron-nuclear resonance. A thorough theoretical analysis was performed by de Gennes *et al.*¹⁰ and it was shown that the strong dependence of the AFMR on the temperature of the nuclear magnetic system is direct evidence of the interaction of the nuclear and ionic spins, leading to a dynamic frequency shift (DFS): to a pulling of their spectra.

Since CsMnBr_3 is an easy-plane antiferromagnetic, one could expect the appearance of a pulling effect in this material too. After we had found the strong distortions of the NMR spectrum due to the dynamic interaction of the electron and nuclear spins (we reported this elsewhere⁷), Zaliznyak and Zorin¹¹ found that in the AFMR spectrum there is a gap, which is also caused by a pulling of the spectral branches. In this paper we compare the results obtained by the NMR and AFMR methods.

Greater absorption of a radio-frequency field, associated with an amplification of the amplitude of the pumping field at the nuclei of the magnetic ions because of the dynamic component H_{hf} of the hyperfine field,⁸ is observed in magnetically ordered crystals. The magnitude of this amplification depends on the form of the AFMR spectrum.

2. CRYSTALLINE AND MAGNETIC STRUCTURE OF THE ANTIFERROMAGNETIC CsMnBr_3

CsMnBr_3 belongs to the large family of binary halides of type ABX_3 , where A is an alkali metal, B is a $3d$ metal, and X is a halogen. The crystal structure is described by the D_{6h}^4 spatial symmetry group with lattice parameters $a = 7.61 \text{ \AA}$ and $c = 6.52 \text{ \AA}$.¹² The Mn atoms in the plane perpendicular to the C_6 axis form a hexagonal lattice.

The crystal lattice determines the specific magnetic structure of this substance, which is determined in experi-

ments on the elastic scattering of neutrons.¹ Because of the fact that the distance between adjacent Mn atoms along the C_6 axis is one-half that in the plane, the exchange interaction integral $J = 214 \text{ GHz}$ determined in neutron scattering experiments,¹³ which characterizes the energy of the antiferromagnetic exchange interaction along the hexagonal axis, is several hundred times J' , which characterizes the antiferromagnetic interaction in the perpendicular plane. The value $J' = 0.46 \text{ GHz}$ is obtained from neutron diffraction data¹³ and $J' = 0.5 \text{ GHz}$ from AFMR data.⁶ At $T_N = 8.3 \text{ K}$, three-dimensional antiferromagnetic ordering occurs in the Mn^{2+} spin system. The anisotropy energy, characterized by the constant D ($D = 2.9 \text{ GHz}^2$ and 2.4 GHz^6), establishes the directions of all spins in the chains perpendicular to the sixth-order symmetry axis. The weak exchange interaction J' between spins lying in one plane leads to the appearance of trigonal 120-degree magnetic structure. Thus, the magnetic structure of CsMnBr_3 can be considered a set of one-dimensional antiferromagnetic chains, elongated along the C_6 axis and interacting weakly among themselves. The unit magnetic cell is shown in Fig. 1a.

Six sublattices form the magnetic structure. Since anisotropy is essentially absent in the basis plane, all of the Mn^{2+} magnetic moments are expanded even in a small constant magnetic field H , applied in the plane, so that the magnetic field direction coincides with one of the bisectors of the triangle (see Fig. 1b and Fig. 2a), i.e., the magnetizations M_1, M_4 will be perpendicular to the field while the other two pairs of sublattices ($M_{2,6}$ and $M_{3,5}$) will form angles of $\pm \pi/6$ with the field direction. On the whole, however, the angles between the directions of adjacent Mn^{2+} spins in the plane will remain close to 120° . Increasing the value of H will lead to a decreasing angle α between the sublattices M_2 and M_3 (the same as for M_5 and M_6), as shown by Chubukov:⁶

$$\cos \frac{\alpha}{2} = \frac{1}{2-z}, \quad z = \frac{H^2}{H_c^2}, \quad (1)$$

with a vanishing in a field $H_c = (48JJ')^{1/2}S \approx 61 \text{ kOe}$ (experimental value⁴ of $H_c \approx 64 \text{ kOe}$ for $T = 1.8 \text{ K}$). Moreover, in each chain a very slight rotation of all spins occurs toward the direction H , which is due to the finiteness of the magnitude of the large exchange interaction field H_E , which is $H_E = 8JS \approx 1500 \text{ kOe}$. Thus, in the magnetic field H_c a col-

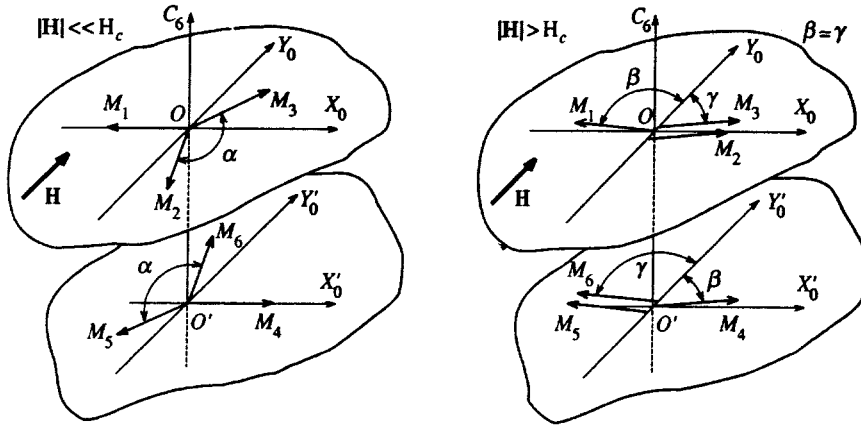


FIG. 2. Schematic representation of the magnetic structure of CsMnBr₃ (a— $H \ll H_c$; b— $H > H_c$).

lapse of two pairs of sublattices occurs (a phase transition of the second kind), and the magnetic structure is transformed from six-sublattice to quasi-two-sublattice (Fig. 2b).

The difference between the angles β and γ is negligible. A further increase in the magnetic field should lead to a rotation of all spins toward the direction of the vector \mathbf{H} until there is a complete breakdown of the antiferromagnetic structure through a spin-flip transition. Measurements of the magnetic moment of CsMnBr₃ as a function of the magnetic field (in fields up to 80 kOe) in Refs. 3 and 4 agree for the most part with theory.⁵

The hyperfine interaction energy per $3d \text{ Mn}^{2+}$ ion in the magnetically ordered state can be written in the form (see Ref. 8)

$$\mathcal{H}_{hf} = A(\langle \mathbf{I} \rangle, \langle \mathbf{S} \rangle), \quad (2)$$

where $\langle \mathbf{S} \rangle$ and $\langle \mathbf{I} \rangle$ are the mean spin of the electron and nucleus of the $^{55}\text{Mn}^{2+}$ ions and A is the hyperfine interaction constant ($A < 0$ for Mn^{2+}). The static field at the nuclei of the $^{55}\text{Mn}^{2+}$ ion (in the absence of an external magnetic field) is

$$\mathbf{H}_{hf} = -\frac{A}{\gamma_n h} \langle \mathbf{S} \rangle, \quad (3)$$

γ_n is the nuclear gyromagnetic ratio ($\gamma_n = 1.06 \text{ MHz/kOe}$ for ^{55}Mn).

Assuming the hyperfine constant A is independent of the sublattice number (and taking into consideration that $A < 0$), the magnitudes of the local fields H_{ni0} , which act on the nuclei of the magnetic ions for all six sublattices, have the form

$$H_{ni0} = |\mathbf{H}_{hf} + \mathbf{H}| = H_{hf} \left(1 + \frac{H^2}{H_{hf}^2} - 2 \frac{H}{H_{hf}} \cos \theta_i \right)^{1/2}, \quad (4)$$

where θ_i is the angle between the external magnetic field vector and the sublattice magnetization. The nuclei of the ions of the sublattices M_1 and M_4 correspond to $i=1$, M_2 and M_5 to $i=2$, and M_3 and M_6 to $i=3$. Let us write the cosines of the angles θ_i in explicit form:

$$\cos \theta_1 = \frac{H}{H_E},$$

$$\cos \theta_2 = \sin \frac{\alpha}{2} + \frac{H}{H_E} \cos^2 \frac{\alpha}{2} + o\left(\frac{H}{H_E}\right),$$

$$\cos \theta_3 = -\sin \frac{\alpha}{2} + \frac{H}{H_E} \cos^2 \frac{\alpha}{2} + o\left(\frac{H}{H_E}\right). \quad (5)$$

Thus, the NMR frequency in CsMnBr₃ in the absence of a dynamic shift is

$$\omega_{ni0} = \gamma_n H_{ni0}. \quad (6)$$

Figure 3 shows the NMR spectrum in CsMnBr₃ (4) predicted by theory (ignoring pulling). For the assumptions made previously, the NMR spectrum in fields $H < H_c$ ($\mathbf{H} \perp C_6$) will consist of three branches. In a field $H > H_c$ the NMR spectrum should consist of one branch because of the very small difference between the angles β and γ (the appearance of the dashed curve 1 in place of the theoretical 1' will be explained below).

3. SAMPLES

The samples were prepared by the Bridgeman method. Fabrication of the CsMnBr₃ crystals has been described in detail elsewhere.⁴ The CsMnBr₃ crystals grown by this method are transparent and are easily cleaved along planes perpendicular to the binary axes. The C_6 axis uniquely determines the intersection of the cleavage planes. The

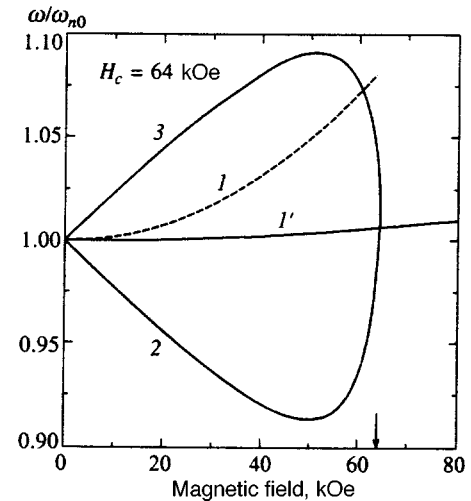


FIG. 3. NMR spectrum of CsMnBr₃ ignoring DFS. 1', 2, 3—branches of NMR spectrum according to Chubukov's angular dependences,⁵ 1—empirical relationship for unshifted frequency of middle branch (see below).

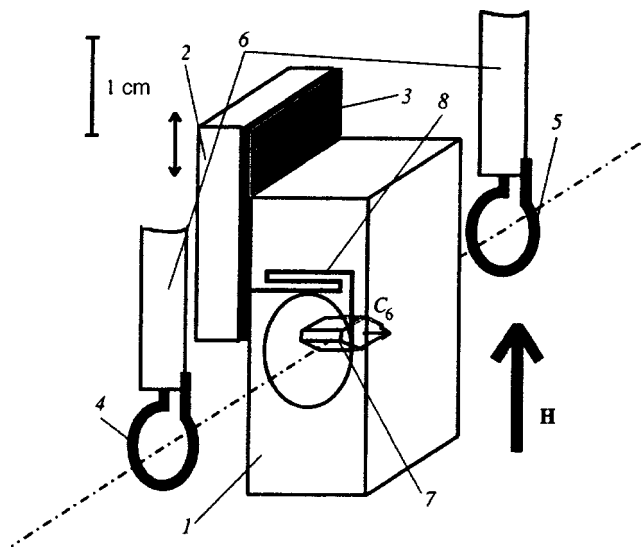


FIG. 4. Resonant circuit: 1—cavity; 2—plate; 3—thin PETE film; 4,5—coupling loops; 6—coaxial feed lines; 7—sample; 8—narrow slot.

CsMnBr_3 crystalline samples are extremely hygroscopic and are hydrated quite rapidly in open air, turning into a white powder that is probably $\text{CsMnBr}_3 \cdot 2\text{H}_2\text{O}$. Therefore, single-crystal samples cleaved from a large crystal were coated with a resin cement. The protective cladding produced in this manner made it possible to work with one CsMnBr_3 single crystal for a long period of time.

4. NMR APPARATUS AND MEASUREMENT PROCEDURE

In view of the strong dependence of the NMR signal on the magnitude of the field \mathbf{H} , a wideband cw decimeter spectrometer of the type described in Ref. 14 with a high- Q cavity was built to investigate nuclear resonance in CsMnBr_3 . The Q of the resonant section in the frequency range investigated was 300–400.

The copper cavity (1 in Fig. 4) was a modified version of a tunable cavity of the “split-ring” type.¹⁵ Three cavities

with differing slot geometry 8 (the size of the gap in the slot is ~ 0.09 mm), in which mica plates were placed to reduce the frequency, were used to cover the range from 500 to 200 MHz. By moving plate 2 one can change the capacitance between plate 2 and cavity 1 (the insulator 3 is a 5–10 μm thick film of polyethylene terephthalate (trade-named Lavsan), thereby changing the resonant frequency. Microwave power is supplied by the coaxial line 6. Coupling to the resonator is accomplished by means of single-turn coils, one of which is the transmitting loop 4, while the other is the receiving loop 5. The diameter of the coupling loops is 5 mm. The direction of the external magnetic field \mathbf{H} , produced by a superconducting solenoid, is indicated in Fig. 4. The C_6 axis of the CsMnBr_3 single crystal 7 was perpendicular to \mathbf{H} . The alignment accuracy of the C_6 axis with respect to the solenoid axis was $\sim \pm 3^\circ$, which did not greatly increase the error in determining the resonant field. The sample was mounted on a special fluoroplastic substrate. The entire system was immersed in a helium bath.

Figure 5 is a block diagram of the spectrometer. The frequency of the microwave oscillator G (a Kh1-43 instrument for studying frequency response) was modulated by the low-frequency ($f=45$ kHz) reference oscillator of the synchronous detector SD2 (PAR 5110 lock-in amplifier). This occurred by mixing the low-frequency signal with the control voltage U_{cont} that sets the frequency of the microwave oscillator. An automatic frequency control (AFC) system, tuned to the first harmonic of the modulation signal, was used to maintain the oscillator frequency at the resonance peak. The AFC system consists of synchronous detector SD1 and a cavity resonance tracker (ETC) with proportional and integral feedback channels.

The output power of the microwave oscillator was less than 3 mW. Absorption in the resonance channel was recorded at the second modulation harmonic U_{s2f} by means of SD2. The depth of the frequency modulation (0.3–3 MHz) was chosen so that it did not greatly broaden the resonant absorption line; it was typically ~ 1.5 MHz.

Attenuators At1 (10 dB) and At2 (10 or 3 dB) were

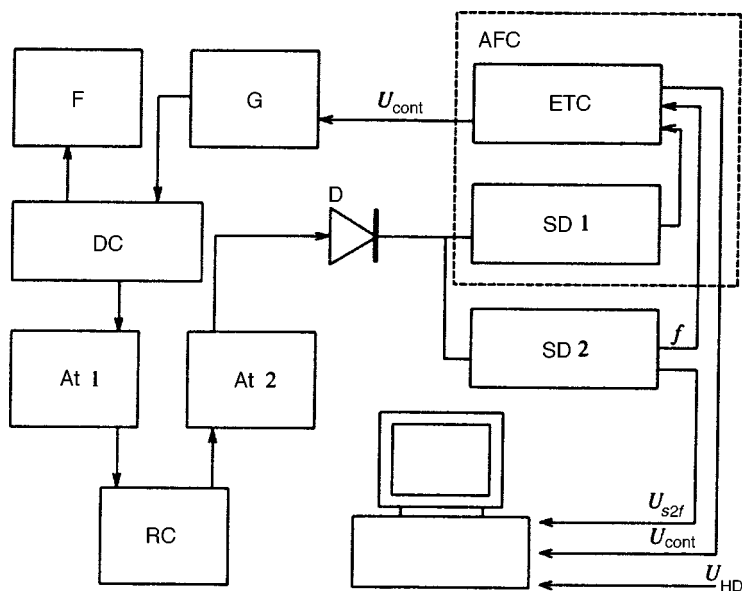


FIG. 5. Block diagram of spectrometer: RC—resonant circuit; G—microwave oscillator; D—detector; SD1—synchronous detector (UNIPAN 232B); SD2—synchronous detector (lock-in PAR 5110); F—Ch3-63/1 frequency meter; At1, At2—attenuators; DC—directional coupler; ETC—electronic tracking circuit; U_{cont} —control voltage; U_{HD} —signal from Hall detector; U_{s2f} —second harmonic signal.

corrected to the input and output of the low-temperature portion of the spectrometer in order to smooth its amplitude–frequency characteristic (AFC). The frequency of the oscillator G was monitored by the frequency meter F (Ch3-63/1), which was connected to the transmitter channel via the directional coupler DC (attenuation of the reflected wave was at least 25 dB).

Thus, the NMR spectrum could be measured in two modes: by scanning the magnetic field at fixed oscillator frequency, or by scanning the frequency at fixed magnetic field. Unfortunately, because of the nonlinearity and poor repeatability of the input line frequency response, this operating mode of the spectrometer could not be fully utilized. Moreover, the sensitivity of the spectrometer turned out to be perfectly adequate in the field-scanning mode. For the first operating mode the error in frequency measurement due to frequency instability of the resonant circuit (Fig. 4) was no greater than 0.1 MHz. The temperature was monitored by means of the resistance of a germanium resistor and the equilibrium saturated vapor pressure of ^4He . Its stability was no worse than ± 0.05 K.

The magnetic field intensity was measured with a Hall detector (U_{HD} in Fig. 5), which together with the CsMnBr_3 sample were located at equivalent positions inside a superconducting solenoid. The error in determining the magnetic field intensity did not exceed 1%.

To excite resonance and to obtain the maximum NMR amplification, the sample was oriented so that the field \mathbf{H} of the solenoid and the radio frequency field \mathbf{h} were mutually perpendicular in the hexagonal plane.

The mass of the CsMnBr_3 single crystals investigated ranged from 50 to 100 mg.

5. SPECTRUM OF COUPLED VIBRATIONS IN CsMnBr_3

Until recently the effect of dynamic interaction of the electron and nuclear systems of the Mn^{2+} ions on the AFMR spectrum was completely ignored during the investigation of the low-frequency resonance properties of the electron system in small-size noncollinear CsMnBr_3 , RbMnBr_3 and CsMnI_3 antiferromagnetics. It was only after the experimental discovery of the pulling of the spectra in CsMnBr_3 (severely distorted NMR spectrum⁷ and gap in the Goldstone branch of the AFMR spectrum¹¹) in Ref. 11 that the spectrum of joint nuclear–electron vibrations was calculated under the assumption that the exchange trigonal structure is not distorted by the field. This condition is satisfied in fields up to ~ 40 kOe. In these fields the formulas of Ref. 11 describe our experimental results satisfactorily.

For a comprehensive description of the results obtained by us over the entire field range up to $H_c = 64$ kOe, we calculated the NMR spectrum using the low-frequency (Goldstone) AFMR mode $\omega_{e1}(H)$ calculated by Chubukov,⁵ which is

$$\omega_{e1}(H) \rightarrow \gamma_e \sqrt{\frac{3}{4}} \frac{H^3}{H_c^2} \quad (7)$$

as $H \rightarrow 0$.

For an easy-plane two-sublattice antiferromagnetic, it is known that its low-frequency vibration occurs with essentially no escape of spin magnetic moments from the easy plane: the ratio of the amplitude of the magnetization vibrations of the sublattices perpendicular to the plane to the amplitude in the plane is H/H_E . A similar relationship must be satisfied in the case of CsMnBr_3 . Limiting consideration to only this vibration, the Lagrangian of the electron spins ζ_{e0} can be written in the form¹⁶

$$\mathcal{L}_{e0} = \frac{1}{2} \frac{\chi_{\parallel}}{\gamma_e^2} (\dot{\phi}^2 - \omega_{e1}^2(H) \phi^2), \quad (8)$$

where ϕ is the small deviation of each spin in the basis plane from the equilibrium direction, and χ_{\parallel} is the susceptibility along the C_6 axis. The quantity $\omega_{e1}(H)$ cannot be given in analytic form. It is the solution of a 6th-degree equation, which can be solved numerically. The form of the given Lagrangian, strictly speaking, is valid as long as no serious deformation of the trigonal magnetic structure occurs. We return to a discussion of this question below.

Typical longitudinal (T_1) and transverse (T_2) relaxation times for the nuclei of the Mn^{2+} ions are $T_1 \sim 1-10$ msec and $T_2 \sim 10$ μsec . These values are clearly several orders of magnitude greater than the period of the natural vibrations of the nuclear magnetization of $^{55}\text{Mn}^{2+}$, which is ~ 2 nsec. For this reason the magnetizations of the nuclear sublattices can be considered as conserving the magnetic moments, and the Lagrangian corresponding to their precession in the field \mathbf{H}_{eff} can be represented in the form proposed for ferromagnetics in the theory of the macroscopic dynamics of magnetic substances.¹⁷ In this case the Lagrangian for the nuclei of one subsystem becomes

$$\mathcal{L}_n = \frac{1}{\gamma_n} (\langle \mathbf{m} \rangle \times \boldsymbol{\Omega} + \gamma_n \mathbf{H}_{\text{eff}}), \quad (9)$$

where $\langle \mathbf{m} \rangle$ is the paramagnetic moment of the sublattice nuclei, $\mathbf{H}_{\text{eff}} = \mathbf{H} + \mathbf{H}_{hf}$ according to Eq. (4) (the dipole field, which does not exceed 2 kOe as a calculation has shown (see below), is ignored here, and $\boldsymbol{\Omega}$ is the angular velocity in spin rotation space.

By adding Eq. (8) and the sum of Eq. (9) for all six sublattices, we obtained the Lagrangian of the system of electron and nuclear spins of the antiferromagnetic being considered with the hyperfine interaction taken into account:

$$\mathcal{L}_{en} = \mathcal{L}_{e0} + \sum_{i=1}^6 \mathcal{L}_{ni}. \quad (10)$$

The characteristic equation of the linearized system (in terms of the small angle of deviation of the spins from equilibrium) of Lagrange equations determines the spectrum of joint vibrations. This equation has the following form for the CsMnBr_3 magnetic structure:

$$\omega_{e1}^2 - \omega^2 = \frac{1}{3} \frac{\omega_{T0}^2}{\omega_{n0}^2} \sum_{i=1}^3 \frac{(\omega^2 + \omega_{ni}^2 - \omega_{ni0}^2) \omega_{ni}^2}{(\omega_{ni0}^2 - \omega^2)},$$

$$\omega_{ni0}^2 = \gamma_n^2 (H_{hf})_i^2 \left(1 + \frac{H^2}{(H_{hf})_i^2} - 2 \frac{H}{(H_{hf})_i} \cos \theta_i \right),$$

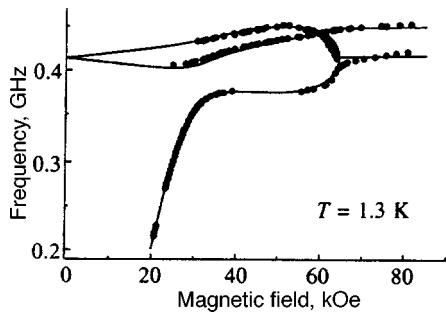


FIG. 6. NMR spectrum of CsMnBr₃: points—experimental NMR spectrum at $T = 1.3$ K, lines—result of calculation using Eq. (11).

$$\omega_{ni}^2 = \gamma_n^2 (H_{hf})_i^2 \left(1 - \frac{H}{(H_{hf})_i} \cos \theta_i \right), \quad (11)$$

where the index i of the spin orientation of the Mn²⁺ ion with respect to the applied field runs through values from 1 to 3, $(H_{hf})_i$ is the value of the hyperfine field for nuclei at the i th position, which at some points, as an experiment has shown, depends on the magnitude of the applied magnetic field, $\omega_{n0} = \omega_{ni0}(H)|_{H=0}$ is the unbiased NMR frequency for any $i = 1, 2, 3$, and $\omega_{T0} = \gamma_e H_{hf} \sqrt{\chi_n / \chi_{\parallel}}$ is the gap in the AFMR spectrum (the formula is exactly the same as in Ref. 11).

As already indicated, the Lagrangian of the electrons can apply rigorously only below 40–45 kOe. However, as will be seen from our experimental results, in fields greater than 50 kOe the dynamical interaction of the electron and nuclear systems almost completely vanishes, and it makes no contribution whatsoever to the solution of Eq. (11). Accordingly, the form of the electron Lagrangian exerts no influence whatsoever on these solutions in strong fields. Thus, the expressions for the NMR frequencies calculated from Eqs. (11) are rigorous in fields below 40 kOe and in fields greater than 50 kOe, but between these values they must be considered empirical approximations.

6. EXPERIMENTAL RESULTS AND DISCUSSION

We observed the NMR lines in a CsMnBr₃ single crystal over the very wide frequency range ~ 200 –450 MHz, in magnetic fields from 20 to 80 kOe. The basic experimental data were obtained at temperatures of 1.3 and 1.75 K. (Observations of the lower branch were also made at $T = 2.5, 3.0, 3.5$ and 4.2 K.) The spectrum at $T = 1.3$ K is shown by the points in Figs. 6 and 7.

a) *Shape of NMR spectrum at $T = 1.3$ and 1.7 K.* In the existence region of the trigonal structure the NMR spectrum splits into three branches, which agrees qualitatively with the form of the spectrum assumed above (see Fig. 3). In fields below 45 kOe, the experimental points indicate that all three branches are severely distorted by the dynamical interaction with the low-frequency AFMR mode. At fields above 50 kOe, where the dynamical shift can be ignored, the upper and lower branches of the spectrum convincingly describe the collapse of the trigonal structure, which is completed, according to other authors, at a field of $H_c = 64$ kOe.

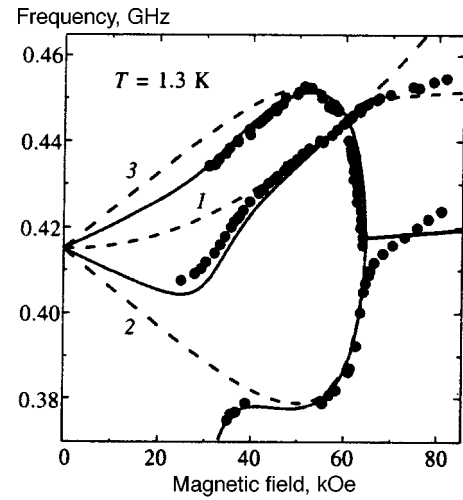


FIG. 7. NMR spectrum of CsMnBr₃ (high frequencies): points—experimental NMR spectrum at $T = 1.3$ K, solid lines—result of calculation using Eq. (11), dashed lines—unbiased NMR spectrum (6) and (12).

The behavior of the middle branch clearly does not agree with the expression for ω_{n10} (6), represented by curve I' in Fig. 3. In order to describe the behavior of this branch it is necessary to assume that H_{hf} for ions of the sublattices perpendicular to the applied field depends on the magnitude of this field. Best agreement with experiment is obtained if this dependence is represented in the form

$$H_{hf}^1 = H_{hf}(1 + cH^2), \quad (12)$$

where $c = 1.9 \times 10^{-5}$ kOe⁻². In Figs. 3 and 7 this empirical dependence is represented by curve I . It agrees with experiment only up to $H = H_c$. We return to a discussion of possible reasons for this anomaly below.

Below 45 kOe the NMR spectrum is distorted by strong dynamical interaction. Our experimental data for all three branches of the spectrum are described very well by the theoretical curves calculated from Eqs. (11) and depicted in Figs. 6 and 7 by the solid curves. Equation (11) contains two parameters ω_{n0} and

$$\omega_{T0} = \gamma_e \frac{\omega_{n0}}{\gamma_n} \sqrt{\frac{\chi_n}{\chi_{\parallel}}}. \quad (13)$$

In this formula χ_n is easily calculated by using the Curie law for nuclear moments. Using the value $\chi_{\parallel} = (1.2 \pm 0.1) \times 10^{-2}$ cgs units/mole from Ref. 4, we see that just one unknown, ω_{n0} , remains in the formula for ω_{T0} . This single parameter was determined from the best fit of the theoretical curves for all three branches of the spectrum (11) to the experimental results. As a result, we obtained $\omega_{n0} = 416 \pm 4$ MHz at $T = 1.3$ K; this frequency corresponds to $H_{hf} = 392 \pm 4$ kOe. Using the value of the hyperfine constant $A = -(1.53 \pm 0.04) \times 10^{-18}$ erg obtained in Ref. 20 from the value of the hyperfine splitting of the EPR line of the Mn²⁺ ion introduced into CsMgBr₃, we determined the mean spin of the Mn²⁺, $\langle S \rangle = |h\omega_{n0}/A| = 1.80 \pm 0.05$. Uncertainty in the value of A , makes the major contribution to the error. From magnetization measurements⁴ at $T = 1.8$ K, $\langle S \rangle = 1.7 \pm 0.1$, which agrees well with our data. From neutron scat-

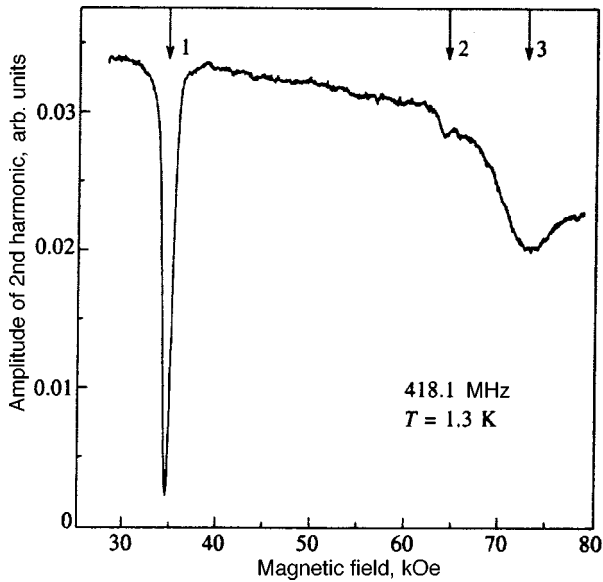


FIG. 8. Example of NMR spectrum at frequency of 418.1 MHz at $T = 1.3$ K. The numbers denote the centers of absorption lines: 1—middle branch, 2—upper branch, 3—signal from collapsing sublattices.

tering work,¹ $\langle S \rangle = 1.5 \pm 0.15$ at $T = 4.2$ K; this also agrees satisfactorily with our value if the difference in temperatures is taken into account.

Using Eq. (13) and our value of ω_{n0} , we have the following relationship for the temperature dependence: $\omega_{T0} = (7.9 \pm 0.4) / \sqrt{T}$ GHz (temperature T in K). Note that the value of ω_{T0} calculated in this manner agrees satisfactorily with the experimental AFMR gap for $T = 1.2$ and $T = 2.0$ K.¹¹

The lower branch 2 undergoes the greatest distortion due to dynamical coupling. The frequency of this branch in the 20–35 kOe interval of magnetic fields varies drastically (of the order of 10 MHz/kOe). The pulling effect is much less evident on the two upper branches, but it is still quite noticeable. This result agrees qualitatively with the results obtained in Refs. 18 and 19, in which collinear antiferromagnetics with two pairs of Mn^{2+} ions located at crystallographically nonequivalent positions were investigated.

The experimental points for $T = 1.7$ K for all branches of the spectrum are essentially identical to the data for $T = 1.3$ K. Only the lower branch at fields below 30 kOe (up to 0.4 kOe) is shifted slightly toward weaker fields; this is a consequence of the temperature dependence of ω_{T0} .

b) *Width and intensity of NMR lines.* The intensity of the absorption lines depends strongly on the magnetic field for all NMR branches.

The signal of the middle branch falls off abruptly with decreasing magnetic field, and at ~ 25 kOe it completely disappears; the same thing also occurs with the upper branch, but at fields below ~ 35 kOe. Such an abrupt falloff in NMR intensity was observed earlier for the upper NMR branch in CsMnF_3 ¹⁸ and CsMnCl_3 .¹⁹ This can be explained by the fact that the nuclear magnetizations precess in antiphase in the different magnetic sublattices. It is quite possible that the same thing also occurs in CsMnBr_3 .

Figure 8 shows an example of the spectrum at 418.1

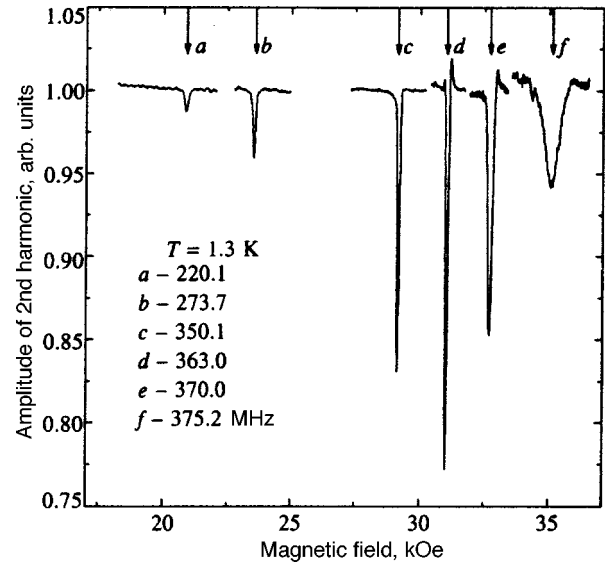


FIG. 9. Experimental low-frequency branch of NMR at $T = 1.3$ K at several frequencies.

MHz. The left line corresponds to the middle branch of the spectrum near maximum intensity. The middle line is the absorption signal of the upper branch near the phase transition. The right line is the signal from two pairs of collapsed sublattices. Note the abrupt increase in absorption intensity for this branch at a field $\sim H_c$.

The lower limit of observations of the low-frequency branch was 197 MHz (the low-frequency limit of the spectrometer); this corresponds to a resonant field of about 20 kOe ($T = 1.7$ K). Figure 9 shows a set of experimental scans of the low-frequency branch at different frequencies. All measurements were made at a fixed modulation amplitude ≈ 0.4 MHz and $Q \sim 400$. Figure 9 convincingly demonstrates the sharp increase in absorption (by more than a factor of 10) of this branch with frequency. Our analysis of the experimental data with $d\omega/dH$ taken into account shows a strong frequency dependence of the width of the resonance line: at about 210 MHz, the width of the absorption line is ~ 4 MHz, and at about 360 MHz it drops to approximately 0.5 MHz.

Note that no peculiarities in the line intensities were observed at the intersection point of the upper and middle branches.

7. ANOMALOUS NMR FEATURES IN CsMnBr_3

a) *Difference in hyperfine fields for different sublattices.* We have already pointed out that in sublattices oriented perpendicular to the applied field, the behavior of the hyperfine field differs from that in other sublattices, even in relatively weak fields. A similar effect in strong fields is even more surprising. According to the existing theory,⁵ in fields greater than H_c CsMnBr_3 is transformed into the quasicollinear state, in which all six sublattices are perpendicular to the applied magnetic field, albeit tilted very slightly toward the latter (cosine of the tilt angle $\sim H/H_E$). Therefore, one might expect that the resonant frequency of the nuclei would be the same in all sublattices. Our results show that this is not the

case. We observed two branches of the NMR spectrum in fields above H_c . The lower branch lies in the frequency range in which one should expect it (near ω_{n10}), extending, as it were, the nonexistent branch I' , although a tendency toward an excess increase beyond H_c is also evident. The upper branch is located 30 MHz above I' . It extends curve I but with a much smaller slope. The presence of two branches means that above H_c , the product $A\langle S \rangle$ is 10% higher for ions in sublattices 1, 4 than in sublattices 2, 6 and 3, 5. Two possible reasons for a change in $A\langle S \rangle$ can be considered:

1. $\langle S \rangle$ can increase with the field because of a decrease in spin reduction, as shown elsewhere.²¹ It is difficult to explain, however, why the effect of the field on spin reduction is different for different sublattice groups, even though they all lie in the same plane and are perpendicular to the applied field.

2. A change in A may be due to a change in the symmetry of the positions of the magnetic ions of sublattices 1, 4. In fields above H_c in each hexagonal layer the spins of one of these sublattices belong to 1/3 of the magnetic ions and are directed opposite the spins of 2/3 of the magnetic ions, which belong to the other two sublattice pairs. As a result, the spins of the first third of the ions are directed opposite the spins of all adjacent ions. For the other two thirds of the ions, the spin directions of adjacent ions alternate (and sum to zero). Moreover, each of the layers has nonzero magnetization. Thus, the hexagonal symmetry of each layer (and of the crystal as a whole) breaks down, and this should be accompanied by magnetostriction. However, at the present time it is difficult to assess the magnitude of this effect and its influence on the constant A . These symmetry considerations might in principle also explain the anomalous behavior of the frequency of the middle branch at fields less than H_c .

We also estimated the possible effect of a change in the dipole field at the nuclei. As numerical calculations showed, the dipole field at the nuclei is nearly unchanged during the collapse of the sublattices. Its total value amounts to about 1.7 kOe, whereas a field of the order of 30 kOe is required to explain the anomaly being considered.

b) *Temperature dependence.* We also found an extremely unusual change in the behavior of the lower branch of the NMR spectrum with increasing temperature. If, for a temperature increase from 1.3 to 1.7 K, the lower branch is shifted, albeit slightly, but in the “required” direction, the lower branch will accordingly be displaced toward weaker fields in accordance with the general prediction that the amount of pulling should decrease with increasing temperature. This effect was observed in all previously investigated collinear antiferromagnetics.

We investigated the behavior of the lower branch of the spectrum at 1.3, 1.7, 2.5, 3.0, 3.5 and 4.2 K. As an example, Fig. 10 shows the experimental data at three temperatures. It is seen that together with the reduction of the NMR frequency at 25 MHz, associated with a 6% decrease in the spontaneous magnetic moment of Mn^{2+} , the lower branch is shifted by about 3 kOe toward larger fields with a temperature increase from 1.7 to 3.5 K. Moreover, the intensity of the NMR signal decreased appreciably, and the resonance line was broadened.

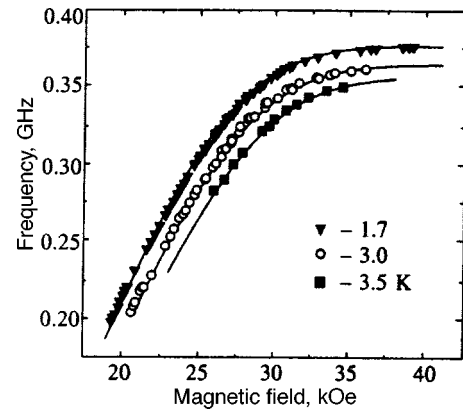


FIG. 10. Temperature dependence of lower NMR branch. Solid lines—result of calculation using Eq. (11) with empirical $F(T)$ function taken into account.

The results indicate that besides the free parameter ω_{n0} (which depends weakly on temperature) and the quantity ω_{T0} (the temperature dependence of which is rigorously defined and shifts the lower NMR branch in the opposite direction), only one quantity—the AFMR frequency ω_{e1} —which should depend on the temperature, remains in Eq. (11), from which the shape of the branches of the NMR spectrum was calculated. We have proposed the following temperature dependence for it:

$$\omega_{e1}(H, T) = \frac{\omega_{e1}(H)}{F(T)}, \quad (14)$$

where $F(T)$ is an empirical function. Then, looking for the best agreement with the experimental curves obtained for the six temperatures stated above using iterative methods, we obtained ω_{n0} and $F(T)$ for these temperatures. Figure 11 shows the function $F(T)$ for various temperatures from 4.2 to 1.3 K. As a result, we have

$$F(T) = 1.0 + 0.1T^2.$$

The equation for $\omega_{e1}(H, T)$, of course, is only valid for fields in which pulling is strong. The temperature at which the NMR line is located at the minimum field is $T_{\min} \approx 1.8$ K. This is thoroughly confirmed by experiment.

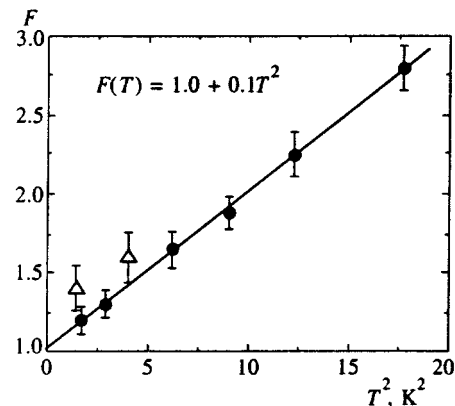


FIG. 11. Empirical $F(T)$ function. Dark points—experimental NMR data, open triangles—fit to AFMR data from Ref. 11.

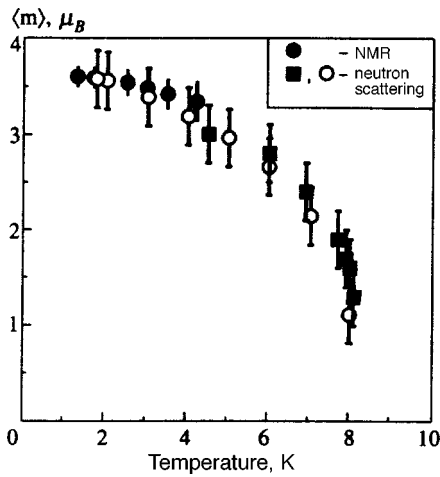


FIG. 12. Temperature dependence of the mean magnetic moment of Mn^{2+} in CsMnBr_3 . Dark points—NMR; squares—from Ref. 1, open points—from Ref. 22.

Figure 12 shows the behavior of ω_{n0} , demonstrating the temperature dependence that we derived for the magnetization of antiferromagnetic sublattices. The data of two neutron diffraction investigations^{1,22} are shown for comparison.

Absolute values are given in Ref. 1, but only relative values in Ref. 22. In the latter case we normalized them to our data at 1.7 K. All results agree to within the error limits.

8. CONCLUSION

In summarizing our work we can point to the following main results:

1. The NMR spectrum in an antiferromagnetic with a trigonal magnetic structure has been investigated for the first time. It has been shown that it is split into three branches and it graphically demonstrates the deformation process of the magnetic triangles with the transition to the quasicollinear structure in a field $H_c = 64$ kOe.

2. The experimental results have made it possible to determine the NMR frequency $\omega_{n0} = 416$ MHz for zero field, and to obtain by means of this value the mean spin of the Mn^{2+} magnetic ion, $\langle S \rangle = 1.80 \pm 0.05$. This means that spin reduction is 28% in quasi-one-dimensional CsMnBr_3 because of quantum fluctuations.

3. At fields below 45 kOe, all three branches of the spectrum experience strong frequency shifts (or pulling) due to the dynamical interaction of the electron and nuclear spin systems. The lower branch is displaced by a particularly large amount (nearly 200 MHz).

4. An equation has been obtained that describes the field dependence of all four modes of the spectrum (three quasi-nuclear and one quasidelectronic), in very good agreement with experiment.

5. Despite expectations, in fields above H_c , where CsMnBr_3 in a first approximation should behave like a collinear two-sublattice antiferromagnetic with one NMR frequency, we found two NMR branches differing by 30 MHz. This can be explained by a disruption of hexagonal symmetry by the field.

6. It is possible that the unexpectedly large increase in resonant frequency with magnetic field at the nuclei of this pair of sublattices, which is perpendicular to the field, is related to the anomaly described in the previous paragraph.

7. The temperature dependence of the location of the low-frequency branch of the spectrum turned out to be more complicated than in three-dimensional magnetic materials. We were able to explain it only by assuming the existence of a rather strong temperature dependence of the frequency of the low-frequency AFMR branch (cubic in the field).

In conclusion, the authors warmly thank A. F. Andreev for assisting in the theoretical portion of this work, and M. I. Krukin, L. A. Prozorova, A. I. Smirnov, S. S. Sosin, and I. A. Fomin for numerous and very fruitful discussions of the results of this work.

This work was partially supported by the Russian Fund for Fundamental Research (Project 95-02-04569-a) and by the U. S. Civilian Research and Development Foundation Program for Independent States of the Former Soviet Union (CRDF, Grant No. RP1-207). A. M. Tikhonov is also grateful to Forschungszentrum Jülich GmbH.

^{*}Deceased.

- ¹M. Eibenschutz, R. C. Sherwood, F. S. L. Hsu, and D. E. Cox, *AIP Conf. Proc.* **17**, 864 (1972).
- ²B. D. Gaulin, T. E. Mason, M. F. Collins, and J. Z. Lavesse, *Phys. Rev. Lett.* **B62**, 1380 (1989).
- ³B. Ya. Kotyuzhaskii and D. V. Nikiforov, *J. Phys.: Condens. Matter* **3**, 385 (1991).
- ⁴S. I. Abarzhi, A. N. Bazhan, L. A. Prozorova, and I. A. Zaliznyak, *J. Phys. Condens. Matter* **4**, 3307 (1992).
- ⁵A. V. Chubukov, *J. Phys. Condens. Matter* **21**, 441 (1988).
- ⁶N. A. Zaliznyak, L. A. Prozorova, and S. V. Petrov, *Zh. Eksp. Teor. Fiz.* **97**, 359 (1990) [*Sov. Phys. JETP* **70**, 203 (1990)].
- ⁷A. S. Borovik-Romanov, S. V. Petrov, A. M. Tikhonov, and B. S. Dumesh, *JETP Lett.* **64**, 225 (1996).
- ⁸E. A. Turov and M. P. Petrov, *NMR in Ferro- and Antiferromagnetics* [in Russian], Nauka, Moscow (1969).
- ⁹A. J. Heeger, A. M. Portis, D. T. Teaney, and G. Will, *Phys. Rev. Lett.* **7**, 307 (1961).
- ¹⁰P. Pincus, P. G. de Gennes, F. Hartmann-Bourtron, and J. M. Winter, *J. Appl. Phys.* **34**, 1036 (1963); P. G. de Gennes, P. Pincus, F. Hartmann-Bourtron, and J. M. Winter, *Phys. Rev.* **129**, 1105 (1963).
- ¹¹I. A. Zaliznyak, N. N. Zorin, and S. V. Petrov, *JETP Lett.* **64**, 473 (1996).
- ¹²J. Goodyear and D. J. Kennedy, *Acta Crystallogr., Sect. B* **28**, 1640 (1974).
- ¹³B. D. Gaulin, M. F. Collins, and W. J. L. Buyers, *J. Appl. Phys.* **61**, 3409 (1987).
- ¹⁴B. S. Dumesh, *Prib. Tekh. Eksp.* **1**, 135 (1986).
- ¹⁵W. N. Hardy and L. D. Whitehead, *Rev. Sci. Instrum.* **52**, 213 (1981).
- ¹⁶M. E. Zhitomirsky, O. A. Petrenko, and L. A. Prozorova, *Phys. Rev. B* **52**, 3511 (1994).
- ¹⁷A. F. Andreev and V. I. Marchenko, *Usp. Fiz. Nauk* **130** (1980) [*Sov. Phys. Usp.* **23**, 21 (1980)].
- ¹⁸L. B. Welsh, *Phys. Rev.* **156**, 370 (1967).
- ¹⁹G. M. Gurevich, B. S. Dumesh, S. V. Topalov, A. V. Andrienko, and A. Yu. Yakubovskii, *Zh. Eksp. Teor. Fiz.* **84**, 832 (1983) [*Sov. Phys. JETP* **57**, 483 (1983)].
- ²⁰G. L. McPherson, R. C. Koch, and G. D. Stucky, *J. Chem. Phys.* **60**, 1424 (1974).
- ²¹M. E. Zhitomirsky and I. A. Zaliznyak, *Phys. Rev. B* **53**, 3428 (1996).
- ²²X. Xu, K. Okada, M. Fujii, N. Wada, M. Kurisu, and S. Kawano, *J. Phys.: Condens. Matter* **8**, L371 (1996).

Translated by Eugene R. Heath